Searching for new borondifluoride β -diketonate complexes with enhanced absorption/emission properties using ab initio tools

Miguel Ponce-Vargas, Bogdan Štefane, Elena Zaborova, Frédéric Fages, Anthony d'Aléo, Denis Jacquemin, Boris Le Guennic

SEARCHING FOR NEW BORONDIFLUORIDE β-DIKETONATE COMPLEXES WITH ENHANCED ABSORPTION/EMISSION PROPERTIES USING *AB INITIO* TOOLS

Miguel Ponce-Vargas[a,b,c], Bogdan Štefane[d], Elena Zaborova[e], Frédéric Fages[e], Anthony D'Aléo[e], Denis Jacquemin*[f] and Boris Le Guennic*[c]

[a] Université Paris-Est, Laboratoire Modélisation et Simulation Multi Echelle, MSME UMR 8208 CNRS, 5 bd Descartes, 77454 Marne-la-Vallée, France.

[b] Institut de Chimie Moléculaire de l'Université de Bourgogne (ICMUB), Université de Bourgogne Franche-Comté (UMR 6302), 9, av. A. Savary, 21078 Dijon, France.

[c] Univ Rennes, CNRS, ISCR (Institut des Sciences Chimiques de Rennes) - UMR 6226, 35000 Rennes, France. E-mail: boris.leguennic@univ-rennes1.fr.

[d] Faculty of Chemistry and Chemical Technology, University of Ljubljana, Večna pot 113, SI-1000 Ljubljana, Slovenia.

[e] Aix Marseille Univ, CNRS, CINaM UMR 7325, Campus de Luminy, Case 913, 13288 Marseille, France.

[f] Laboratoire CEISAM, UMR CNRS 6230, Université de Nantes, 2 Rue de la Houssinière, BP 92208, 44322 Nantes Cedex 3, France; E-mail: Denis.Jacquemin@univ-nantes.fr.

ABSTRACT

The rational design of fluorophores with enhanced absorption/emission properties increasingly relies on theoretical chemistry, as new *ab initio* methods suited for electronically excited-states reduce the gap between calculated and experimental results. In this framework, Time-Dependent Density Functional Theory (TD-DFT) emerges as an attractive option as it often provides accurate results at a moderate computational cost. Here, we perform a TD-DFT-SOS-CIS(D) study of a panel of 18 borondifluoride β-diketonate complexes that can be classified as: curcuminoids, hemicurcuminoids, their ethynylene analogues, and 2'-hydroxy-chalcones. First, we reproduce the experimental 0-0 energies with refined models considering the impact of vibrational and solvent effects, the latter through both linear response and two-state specific approaches. We also evaluate the impact of double excitations by using the SOS-CIS(D) scheme to correct the TD-DFT estimates. In addition, we carry out a vibronic simulation for a representative system. Next, we analyze the obtained key structure-property relationships leading to pronounced bathochromic shifts, and finally, based on the obtained results, we propose a panel of related compounds looking for systems with absorption and emission maxima located at longer wavelengths.

INTRODUCTION

The design of fluorescent dyes is a subject of paramount importance for the development of molecular probes for biomedical imaging and emitting solid-state materials for display technologies[1-8]. Among the numerous families of organic luminescent molecules, boron dipyrromethene (BODIPY) derivatives (Scheme 1) are the most widely used owing to their outstanding photophysical properties and very large emission quantum yields[9-13]. Another interesting family also displaying a tetra-coordinated boron core is that of the borondifluoride β-diketonate complexes (Scheme 1). They present high photoluminescence in both solution and solid states[14-17], develop significant cross section for two-photon absorption[18,19], and exhibit good environmental stability upon light irradiation[20].

In typical borondifluoride β-diketonate structures, the introduction of one or more electron donor organic fragments (D) connected by a π-conjugated segment to the acceptor dioxaborine moiety (A) leads to the generation of push-pull D-π-A or quadrupolar-like D-π-A-π-D molecules. As a consequence, the lowest-energy absorption and emission bands display a significant intramolecular charge transfer (CT) character[16,21] which allows a fine tuning of the optical properties, depending on the strength of the donor group, e.g., the absorption and emission maxima are redshifted when strong *pushing* groups are used[22]. In addition, a wide gap between absorption and emission maxima, that is a large Stokes shift, is desired for many practical applications, as it allows to reduce losses arising from self-absorption[23]. Among the different strategies used to induce both bathochromic shifts and enhanced Stokes shifts, the incorporation of electron donor groups[24-26] and the extension of the π-conjugation path[27-29] have proven to be particularly effective.

A key parameter in the theoretical study of all dyes is the 0-0 Energy (E^{0-0}) that can be defined as the difference between the excited state (ES) and ground state (GS) energies

taken at their respective optimal geometries and corrected for the difference of zero-point vibrational effects. This value can be calculated and compared with the experimental crossing point between absorption and fluorescence profiles (AFCP). In this general framework, Time-Dependent Density Functional Theory (TD-DFT) -which determines the response of the electron density to a perturbation from an external electric field- represents a useful tool, as it allows for an efficient determination of all key ES properties, notably geometries and vibrational signatures. However, for many borondifluoride complexes, it has been shown that TD-DFT tends to provide too large transition energies[30], an error that can be reduced by the incorporation of corrections for double excitations, with methods such as CIS(D)[31], SCS-CIS(D)[32], SOS-CIS(D)[32], ADC(2)[33] and CC2[34]. The CIS(D) method provides a perturbative correction to the CIS energy, similarly to what second–order Møller–Plesset (MP2) theory does for GS[35], whereas the SCS-CIS(D) variant employs two parameters to scale the two spin components of the direct term of CIS(D) starting from the two-parameter spin-component scaled (SCS) MP2 GS. By scaling the opposite-spin direct term of CIS(D) only, starting from the one-parameter scaled opposite-spin (SOS) MP2 GS, one obtains the SOS-CIS(D) approach[32]. This last approach has been shown to be efficient for BODIPY dyes and their aza derivatives[36], BODIPY-cyanines[37], ladder-type-π-conjugated dyes[38], as well as BOPHYs[39].

Herein we perform a detailed TD-DFT study of the relationships between absorption/emission properties and structural features of a large set of borondifluoride β-diketonate complexes based on four families of dyes: curcuminoids[40], hemicurcuminoids[41,42], their ethynylene analogues[41] and 2'-hydroxy-chalcones (Scheme 2)[43-45]. As a first step, we calculate the AFCP values by using an adiabatic TD-DFT protocol, taking into account solvent effects through a refined PCM model, and accounting for double excitations through the SOS-CIS(D) approach. Additionally, we carried out a vibronic analysis within the Franck-Condon approximation, and we use electronic density difference (EDD) maps and charge-

transfer parameters to describe the ES nature of the considered dyes. Finally, we use all the obtained information to propose novel structures of borondifluoride β-diketonate complexes with improved absorption/emission properties.

COMPUTATIONAL DETAILS

All DFT/TD-DFT calculations were carried out with the Gaussian09 code[46], tightening self-consistent field convergence thresholds (10^{-10} a.u.). For all the calculations the M06-2X[47] functional was employed, given its good performance in adiabatic energy calculations of chromophores with O-B-O central linkages[36-38]. We verified the stability of the GS and ES geometries by vibrational frequency calculations. Two atomic basis sets, 6-31G(d) for geometry optimizations and frequency calculations, and 6-311+G(2d,p) for electronic transitions were applied. We consider the Polarizable Continuum Model (PCM) in order to reproduce the solvation effects (here dichloromethane) on the spectral properties. In this model, the solvent is represented by a polarizable continuum medium characterized by its dielectric permittivity ε and other macroscopic parameters, whereas the solute, by a charge distribution inside a solvent cavity[48,49]. For all geometry optimizations, we considered an *equilibrium* limit, whereas for calculating absorption and emission energies we employed the *nonequilibrium* limit. In the framework of excited-state calculations with PCM[50], several models are available. On the one hand, one can select the Linear Response (LR)[51,52] formalism, in which the transition density is used to estimate solvent effect on ES properties, an approach well suited for local ES. On the other hand, one can select one of the State-Specific (SS) formalism, that use the one-particle density matrix to correct the gas-phase transition energies, a scheme suited for CT ES. Two SS models are available in Gaussian: the iterative one of Improta and co-workers[53], simply referred to as "SS" in the following, and the perturbative corrected Linear Response (cLR)[54] method of Mennucci and coworkers. Here we applied these methodologies, also including for all of them, the configuration interaction correction in its scaled opposite spin form [SOS-CIS(D)][32].

The scaled opposite spin form [SOS-CIS(D)] calculations have been computed with the *Q-Chem* package[55] applying 6-311+G(2d,p) basis set and the resolution of the identity scheme, with a triple-ζ auxiliary basis set.

For a representative system, the vibrationally resolved optical spectra within the harmonic approximation were computed by using the FC classes program on the basis of TD-DFT vibrational signatures[56-59]. We applied the FC approximation and simulated the spectra by using a convoluting Gaussian function presenting a half width at half-maximum (HWHM) of 0.05 eV to allow direct comparison with the experiment. A maximal number of 25 overtones for each mode and 20 combination bands for each pair of modes were included in the calculation. The maximum number of integrals computed for each class was set to 10^6.

Additionally, to visualize the electronic density redistribution and the possible intramolecular CT we used the difference between the total densities of the excited and ground states as provided by TD-DFT. All $\Delta\rho(r)$ (that is the EDD plots) as well as all HOMO-LUMO isosurfaces have been plotted with the Chemcraft code[60], considering a contour threshold of 0.004 a.u. for the former and 0.03 a.u. for the latter. Additionally, the amount of CT (q^{CT} in |e|), CT distance (d^{CT} in Å), and CT dipole (μ^{CT} in Debye) have been calculated according to the methodology proposed by Le Bahers and coworkers[61,62], in order to quantify the electronic redistribution induced by the excitations.

RESULTS AND DISCUSSION

Assessment of the theoretical approaches

In previous works dealing with the modeling of optical properties of (aza-)BODIPY and related derivatives, the efficiency of the PCM-TD-DFT-SOS-CIS(D) protocol has been proven[36-39], providing us a guideline for the present calculations. Nevertheless, we test three protocols here, in order to pinpoint the best option for the investigated dyes. We can classify the studied systems as: curcuminoids (**1**)[40], characterized by two donor groups attached to a dioxaborine moiety through π-conjugated chains, hemicurcuminoids (**2**)[41,42], with one donor group connected to the dioxaborine fragment by a π-connector while the other one is linked through a single bond; their ethynylene analogues (**3**)[41], and 2'-hydroxy-chalcones (**4**)[43-45]. In Scheme 2, we can observe the complete panel of borondifluoride β-diketonate complexes studied in the first stage of this work.

The experimental AFCP energies and the corresponding theoretical values are listed in Table 1, and the results of a statistical analysis including mean absolute error (MAE), mean square error (MSE), standard deviation (SD), maximal positive and negative deviations [Max(+) and Max(-)], as well as theory/experiment linear determination coefficients (R^2), are given in Table 2. Additionally, we present a graphical comparison between theoretical results and experimental data in Figure 1. Such analysis reveals that without considering SOS-CIS(D) corrections, the LR-PCM solvent model allows to reproduce more consistently the experimental data trend, as evidenced by its higher R^2 value of 0.954 in comparison to the 0.932 and 0.916 R^2 values obtained with cLR and SS, respectively. In all cases, the incorporation of SOS-CIS(D) terms improves the experiment/calculation correlation, with higher R^2 values of 0.959 for LR-SOS-CIS(D), 0.978 for cLR-SOS-CIS(D), and 0.956 for SS-SOS-CIS(D). One therefore notices that the cLR-SOS-CIS(D) approach delivers the most

consistent evaluation, which is important as we aim to design new compounds (*vide infra*). Turning now to the MSE and MAE that indicate how close our values are from experimental data, it seems that the incorporation of SOS-CIS(D) correcting terms has a positive influence, irrespective of the selected solvation model. Indeed, the MAE goes from 0.162 eV to 0.057 eV for LR, from 0.329 eV to 0.112 eV for cLR, and from 0.291 eV to 0.074 eV for SS, whereas the MSE diminishes as well (see Table 2). All this MAE, close or below 0.1 eV are very satisfying, as the typical errors of TD-DFT for dyes are in the 0.2-0.3 eV range. As cLR-SOS-CIS(D) is the most effective approach in the experimental data tendency, it seems interesting to determine for which family of compounds belonging to our data set, this protocol is the most accurate. For curcuminoid derivatives, this approach presents a determination coefficient of 0.996 followed by hemicurcuminoid with 0.965, and ethynylene-hemicurcuminoid with 0.947. As the cLR-SOS-CIS(D) protocol has also proved to be an efficient methodology for accurately estimating the AFCP values of BODIPY dyes and their aza-derivatives[36], BODIPY-cyanines[37], ladder-type-π-conjugated dyes[38], and BOPHYs[39], we have selected it in the following.

Analysis of the band topology

We investigated the vibronic couplings of one representative example, namely **1T-NMe$_2$**, in order to unravel the origin of the specific band shapes of these dyes. As the investigated transition is significantly dipole-allowed, we applied the Franck-Condon approximation (see Computational details). The simulated absorption and emission spectra as long as their experimental counterparts are shown in Figure 2. Apart from the fact that a deconvolution of both spectra has been performed, it is clear that there exists an acceptable agreement between theory and experiment in terms of absorption and emission maxima positions. We have analyzed the key vibronic transitions responsible for the band shapes, and

for the emission spectra. We found that the main vibrational mode corresponds to a symmetric stretching of the lateral aromatic rings and the vinyl bridges, with a minor contribution from the *meso* phenyl. For the UV/vis absorption case, an additional contribution of the C-N stretching involving the aromatic rings and the appended nitrogen atoms can be noticed, which notably explains the presence of the intense secondary absorption peak at 550 nm, clearly recognizable in the calculated deconvoluted spectrum.

Structure-spectrum relationships

It is well established that the planarity of the chromophores tunes their optical properties, as it influences the magnitude of the π-conjugation[63]. For this reason, the dihedral angles between the borondifluoride core and the *meso* substituent in **1T-OMe** and **1T-NMe$_2$** have been calculated (see Figure 3 and Table 4), and some rather large values (both in GS/ES) are obtained (70.7°/55.5° for **1T-OMe** and 74.7°/61.0° for **1T-NMe$_2$**), suggesting a limited π-conjugation between the acacBF$_2$ core and the *meso*-group.

The HOMO-LUMO plots corresponding to five compounds representative of each category are shown in Figure 4. In all cases, the LUMO is mainly located on the boron difluoride moiety confirming that it acts as an acceptor, whereas the HOMO is spread over the lateral substituents, which act as electron density sources, that is, as donor groups. As expected, the presence of an acetonaphthone fragment in **4Naph-OMe** results in a more extended HOMO in the bottom part of the molecule, in comparison to **3-OMe**.

By using the AFCP values, charge-transfer parameters, and density difference plots (see Table 3 and Figure 5), one can establish a relationship between the absorption/emission properties and the electronic features of the studied chromophores. For instance, with respect to curcuminoids, the plot of the electronic density difference (EDD, Figure 5) shows an electronic density flux from the lateral arms toward the acacBF$_2$ moiety, whereas the *meso*-

substituent contributes to a (much) smaller extent to the excited-state, which can be associated to the minor conjugation between the central core and the *meso* ring (see above). Moreover, replacing the methoxy groups in **1-OMe** by the stronger *N*,*N*-dimethylamino leading to **1-NMe$_2$** results in pronounced redshifts of ca. -0.477 eV (-0.435 eV) experimentally (theoretically), evidencing the close relationship between the electron donor strength of the lateral groups and the absorption/emission maxima displacements. This is corroborated by the q^{CT} values of 0.575|e$^-$| for **1-OMe** and 0.649|e$^-$| for **1-NMe$_2$**, as well as the EDD maps that shows the major electronic density variations caused by the *N*,*N*-dimethylamino groups. Similar bathochromic displacements of -0.440 eV (-0.374 eV) are obtained by experiment (theory) for the **1T-OMe/1T-NMe$_2$** pair.

Interestingly, the ethynylene hemicurcuminoids (**3-Ph** and **3-OMe**, **3OMe-Ph** and **3OMe-Cl**) display the smallest charge transfer values of the considered borondifluoride β-diketonate complexes. This is consistent with the fact that the EDD maps reveal that such charge comes mainly from the aromatic substituent connected to the ethynyl linker, while the tetrahydronaphthalene moiety contribution is rather small. Moreover, the incorporation of electron donor methoxy groups in both the tetrahydronaphthalene fragment (**3OMe-Ph**) or the ethynyl phenyl group (**3-OMe**) of **3-Ph**, causes no significant bathochromic shifts.

The common feature of chromophores **3-Ph** and **3Ph-t-Ph** is the phenylethynyl group linked to the borondifluoride core. By using these compounds, one can evaluate the impact of the 1-hydroxy-1,2,3,4-tetrahydronaphthalene moiety (**3-Ph**) on the absorption/emission properties with respect to a single-bonded phenyl group (**3Ph-t-Ph**). We found that the presence of the tetrahydronaphthalene ring generates a considerable red shift of ca. -0.212 eV (-0.291 eV) in the measured (calculated) AFCP with respect to **3Ph-t-Ph**. This outcome might be explained by the shorter charge transfer distance found in **3-Ph** (0.899 Å) than in **3Ph-t-Ph** (1.432 Å).

Finally, the 2'-hydroxy-chalcones **4Ph-OMe** and **4Naph-OMe** enable us to evaluate the influence of the aromatic groups (acetophenone and acetonaphthone, respectively) fused with the borondifluoride moiety, in the spectral properties. Then, **4Naph-OMe** exhibits a red-shift of -0.184 eV (-0.234 eV) in comparison to chromophore **4Ph-OMe** when considering experimental data (theoretical ones). This can be justified by the relevant contribution of the acetonaphthone fragment to the charge transfer (see EDD), and we also notice that the charge transfer distance attains 0.751 Å in **4Naph-OMe** with is much smaller than the 1.958 Å value determined in **4Ph-OMe**.

Toward the design of new compounds

The above-mentioned results encouraged us to apply the cLR-SOS-CIS(D) protocol to predict not-yet-synthesized borondifluoride *β*-diketonates, in the hope to define some structures with smaller AFCP values, thanks to the addition of strong electron donor -NMe_2 groups, also displaying ethynyl connectors. Additionally, we evaluate the effect of electron withdrawing -NO_2 and -CN groups in order to explore the possibility to reverse the push-pull direction of the hypothetical structures. For all the proposed systems (Scheme 3), AFCP values, have been determined, and subsequently, by linear regression using the data of Table 1, the theoretical best estimates can be obtained. These data are presented in Table 5.

The impact of incorporating a *N*,*N*-dimethyl aminophenyl group through an ethynyl linker to the *meso* position of **1-OMe** is manifested in chromophore **VI-NMe_2**, where the lowest AFCP value of the hypothetical series, *i.e.* 1.730 eV, is found. Its EDD map evidences how the ethynyl linker allows an effective conjugation of the *N*,*N*-dimethylaminophenyl moiety, and also plays a relevant role in the ES. In Table 5 we can observe the fivefold increase of the charge transfer dipole (11.719 D) of **VI-NMe_2** with respect to **1-OMe** (2.293

D), in line with the (much) stronger push-pull behavior of the *meso* moiety in the proposed compound.

Remarkably, the combination of the tetrahydronaphthalene borondifluoride core with electron withdrawing groups through ethynyl linkers enables to obtain modified 2'-hydroxychalcones, with very small AFCP values. Indeed, the best estimates for **III-NO_2** and **III-CN** AFCP energies are 2.001 eV and 2.057 eV, respectively. One can analyze this fact, as a consequence of the reverse CT induced by the electron-withdrawing -NO_2 and -CN groups, that attract so efficiently the electron density from the boron difluoride core that the acetonaphthol fragment now plays the role of main electron donor group (Figure 6), thus leading to an enhanced polarization. This fact is also reflected by the larger charge transfer dipoles of 10.09 D and 9.08 D found in for **III-NO_2** and **III-CN**, respectively. This effect is also plausible in **IV-NO_2**, where the acetophenone moiety acts as electron donor group. For that compound, theory also predicts a very red-shifted spectra (AFCP of 2.194 eV) as well as a large charge transfer dipole (8.31 D). Of course, the replacement of the nitro group by the electron donor *N*,*N*-dimethylamino strongly modifies the excitation nature of the system. Indeed, in **IV-NMe_2**, the acetophenone-acacBF_2 region becomes, as expected, the electron density acceptor, and this leads to an AFCP of 2.091 eV, accompanied by a very strong charge transfer dipole of 19.11 D, with almost one electron being transferred upon absorption of light.

Finally, the **II-NMe_2** compound, analogous to **1T-NMe_2**, but with ethynyl linkers, presents an AFCP of 2.071 eV, which remains quite low though it is blue shifted by +0.164 eV compared to its already synthesized parent.

CONCLUDING REMARKS

The theoretical calculation of the adiabatic excited-state energies through a protocol including both, solvent effects thanks to the polarizable continuum model, and the impact of double excitations through a perturbative correction, has proved to be able to reproduce the evolution of the absorption fluorescence crossing points (AFCP) of a large series of borondifluoride β-diketonate complexes, with good accuracy and at a reasonable computational cost. Overall, it is the cLR-SOS-CIS(D) approach that gives the most accurate trend, that is, that provides the largest determination coefficient with respect to experiment (R^2=0.978); other schemes, such as LR-SOS-CIS(D) and SS-SOS-CIS(D) deliver smaller mean absolute deviation with respect to experiment but at the cost of slightly poorer correlation. As expected for fluoroborate derivatives, we also found that TD-DFT AFCP energies are significantly too large, irrespective of the considered solvent model, so that the corrections brought by SOS-CIS(D) are indeed mandatory to obtain reasonably accurate estimates.

By using as qualitative indexes the charge-transfer characteristics as well as the electronic density difference plots, we acquired a deeper understanding of the observed bathochromic shifts and of their relationships with the structural features. With all this information, we have proposed a complete set of structurally related-systems, and then calculated their AFCP values. The hypothetical systems displaying the lowest AFCP values are the curcuminoids containing a strong electron donor $–NMe_2$ group linked to the *meso* position through an ethynyl linker; and the modified 2'-hydroxychalcones, displaying ethynyl linkers. Interestingly, in the latter family, we can reverse the charge-transfer direction, by introducing electron donor or electron withdrawing groups, obtaining in both cases large charge transfer dipoles leading to low AFCP values. It is our hope that this work will

stimulate additional experimental research in the field, as it seems clear that the most redshifted systems remain to be synthesized.

ACKNOWLEDGMENTS

M.P.-V. thanks the ANR (Project ANR-14-CE05-0035-02) for his postdoctoral grant. D. J. acknowledges the European Research Council (ERC) and the Région des Pays de la Loire for financial support in the framework of a Starting Grant (MARCHES-278845) and LumoMat Project, respectively. This research used resources of the Centre de Calcul Intensif des Pays de Loire (CCIPL), a local Troy cluster, and the GENCI-CINES.

FIGURES AND TABLES

Table 1. Experimental AFCP energies (eV) and their corresponding calculated values.

	AFCP (eV)						
	Exp[a].	Calc.					
		LR	cLR	SS	LR-SOS-CIS(D)	cLR-SOS-CIS(D)	SS-SOS-CIS(D)
1-OMe	2.423	2.595	2.831	2.801	2.346	2.582	2.552
1T-OMe	2.347	2.532	2.756	2.723	2.255	2.480	2.447
1-NMe_2	1.946	2.260	2.464	2.408	1.943	2.147	2.091
1T-NMe_2	1.907	2.228	2.454	2.380	1.880	2.106	2.032
2-OMe	2.828	2.994	3.259	3.200	2.656	2.921	2.862
2-SMe	2.655	2.834	3.075	3.001	2.612	2.852	2.778
2-anul	2.456	2.775	3.002	2.870	2.392	2.620	2.487
2-NMe_2	2.327	2.645	2.913	2.832	2.213	2.481	2.400
2Ph-OMe	2.621	2.814	3.058	2.984	2.497	2.740	2.667
2CF_3-OMe	2.595	2.846	3.120	3.075	2.423	2.696	2.652
2Ph-d-Ph	2.957	3.004	3.255	3.237	2.766	3.016	2.999
3Ph-t-Ph	3.022	3.156	3.362	3.299	3.027	3.233	3.170
3-Ph	2.810	2.950	3.131	3.110	2.736	2.917	2.896
3-OMe	2.647	2.855	3.040	2.949	2.627	2.812	2.721
3OMe-Cl	2.747	2.870	3.054	3.019	2.653	2.836	2.802
3OMe-Ph	2.721	2.890	3.075	3.039	2.660	2.845	2.809
4Ph-OMe	2.477	2.792	3.038	3.110	2.466	2.712	2.784
4Naph-OMe	2.293	2.633	2.798	2.735	2.312	2.478	2.414

[a] Experimental data from ref. 40-45.

Table 2. Statistical analysis obtained from comparison of experimental and theoretical AFCP energies (Table 1): mean absolute error (MAE), mean square error (MSE), standard deviation (SD), maximal positive and negative deviations [Max(+) and Max(-)], and theory/experiment linear determination coefficients (R^2). All values except those for R^2 are given in eV.

	MAE	MSE	SD	Max(+)	Max(-)	R^2
LR	0.162	0.040	0.243	0.339	0.047	0.954
cLR	0.329	0.151	0.246	0.586	0.298	0.932
SS	0.291	0.120	0.255	0.633	0.272	0.916
LR-SOS-CIS(D)	0.057	0.007	0.287	0.019	-0.191	0.959
cLR-SOS-CIS(D)	0.112	0.019	0.285	0.235	0.059	0.978
SS-SOS-CIS(D)	0.074	0.010	0.295	0.307	0.031	0.956

Table 3. Experimental Absorption maxima (nm), emission maxima (nm), Stokes shift (cm^{-1}), and calculated charge transfer ($|e^-|$), charge transfer distance (Å), and charge transfer dipole (Debye).

	Abs. max[a]. (nm)	Em. max[a]. (nm)	Stokes shift[a] (cm^{-1})	Charge transferred ($|e^-|$)	Charge transfer distance (Å)	Charge Transfer Dipole (Debye)
1-OMe	488	538	1904	0.575	0.830	2.293
1T-OMe	505	554	1751	0.565	0.798	2.169
1-NMe_2	597	683	2109	0.649	1.002	3.127
1T-NMe_2	613	692	1862	0.640	0.868	2.667
2-OMe	407	475	3517	0.483	2.384	5.530
2-SMe	423	521	4447	0.528	3.151	7.991
2-anul	463	555	3580	0.554	3.153	8.395
2-NMe_2	501	569	2385	0.520	2.856	7.139
2Ph-OMe	444	506	2760	0.513	2.513	6.187
2CF_3-OMe	448	512	2790	0.485	2.576	6.006
2Ph-d-Ph	398	443	2552	0.454	1.513	3.300
3Ph-t-Ph	401	420	1128	0.464	1.432	3.193
3-Ph	431	452	1078	0.438	0.899	1.891
3-OMe	446	493	2138	0.501	1.990	4.783
3OMe-Cl	430	475	2203	0.466	1.065	2.385
3OMe-Ph	443	469	1251	0.462	1.136	2.519
4Ph-OMe	455	556	3992	0.569	1.958	5.349
4Naph-OMe	486	609	4156	0.537	0.751	1.938

[a] Experimental data from ref. 40-45

Table 4. Selected dihedral angles for the studied chromophores (degrees). See Figure 3 for definition of the angles.

Dihedral		1-OMe	1-NMe_2	1T-OMe	1T-NMe_2	2-OMe	2-SMe	2-anul	2-NMe_2	2CF_3-OMe
< a-b	GS	2.466	2.24	0.65	0.86	3.01	2.71	2.79	2.63	2.19
	ES	1.63	1.68	0.99	0.54	1.38	1.30	1.33	1.53	1.22
<b-c	GS	1.469	0.93	1.80	1.00	0.76	0.34	0.82	0.73	1.11
	ES	0.56	0.57	1.12	0.82	0.01	0.28	0.04	0.11	1.17
< a-d	GS	-	-	70.70	74.69	-	-	-	-	-
	ES	-	-	55.53	61.04	-	-	-	-	-
Dihedral		2Ph-OMe	2Ph-d-Ph	3Ph-t-Ph	3-Ph	3-OMe	3OMe-Cl	3OMe-Ph	4Ph-OMe	4Naph-OMe
< a-b	GS	2.83	2.87	-	4.12	1.90	3.32	0.71	6.43	6.08
	ES	1.28	1.35	-	1.82	0.74	1.78	0.31	2.40	3.38
< b-c	GS	1.40	2.35	-	-		-	-	1.02	0.76
	ES	0.50	0.70	-	-		-	-	0.93	0.37
< a-d	GS	16.34	15.90	14.58	-		-	-	-	-
	ES	5.20	4.30	4.41	-		-	-	-	-
< a-c	GS	-	-	3.41	-		-	-	-	-
	ES	-	-	2.20	-		-	-	-	-

Table 5. AFCP energies (eV) obtained with cLR and cLR-SOS-CIS(D), best estimates obtained by linear regression using the cLR-SOS-CIS(D) AFCP values of Table 1, charge transfer ($|e^-|$), charge transfer distance (Å), and charge transfer dipole (Debye), for a set of hypothetical borondifluoride *β*-diketonate complexes.

	cLR	cLR-SOS-CIS(D)	Best estimates	Charge transferred ($|e^-|$)	Charge transfer distance (Å)	Charge Transfer Dipole (Debye)
I-CN	3.143	3.136	3.013	0.463	0.831	1.849
II-CN	2.733	2.611	2.457	0.568	1.312	3.581
III-CN	2.530	2.235	2.057	0.613	3.086	9.083
IV-CN	2.796	2.423	2.256	0.622	2.513	7.508
V-CN	3.362	3.296	3.184	0.434	0.652	1.359
VI-CN	2.627	2.370	2.200	0.552	1.571	4.163
I-NMe_2	2.546	2.378	2.209	0.634	1.596	4.862
II-NMe_2	2.478	2.248	2.071	0.608	1.550	4.528
III-NMe_2	2.690	2.408	2.240	0.547	2.373	6.232
IV-NMe_2	1.713	2.267	2.091	1.057	3.763	19.105
V-NMe_2	2.488	2.597	2.441	0.800	4.177	16.056
VI-NMe_2	2.052	1.927	1.730	0.746	3.269	11.719
I-NO_2	3.169	3.134	3.012	0.461	0.474	1.049
II-NO_2	2.693	2.567	2.409	0.590	1.191	3.371
III-NO_2	2.480	2.182	2.001	0.627	3.351	10.087
IV-NO_2	2.753	2.364	2.194	0.639	2.708	8.313
V-NO_2	3.343	3.282	3.169	0.447	0.816	1.751
VI-NO_2	2.641	2.381	2.212	0.554	1.482	3.941

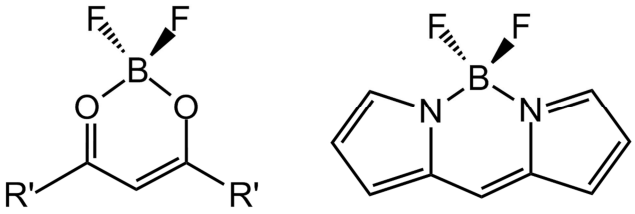

Scheme 1. Representation of a borondifluoride β-diketonate complex (left) and a BODIPY (right).

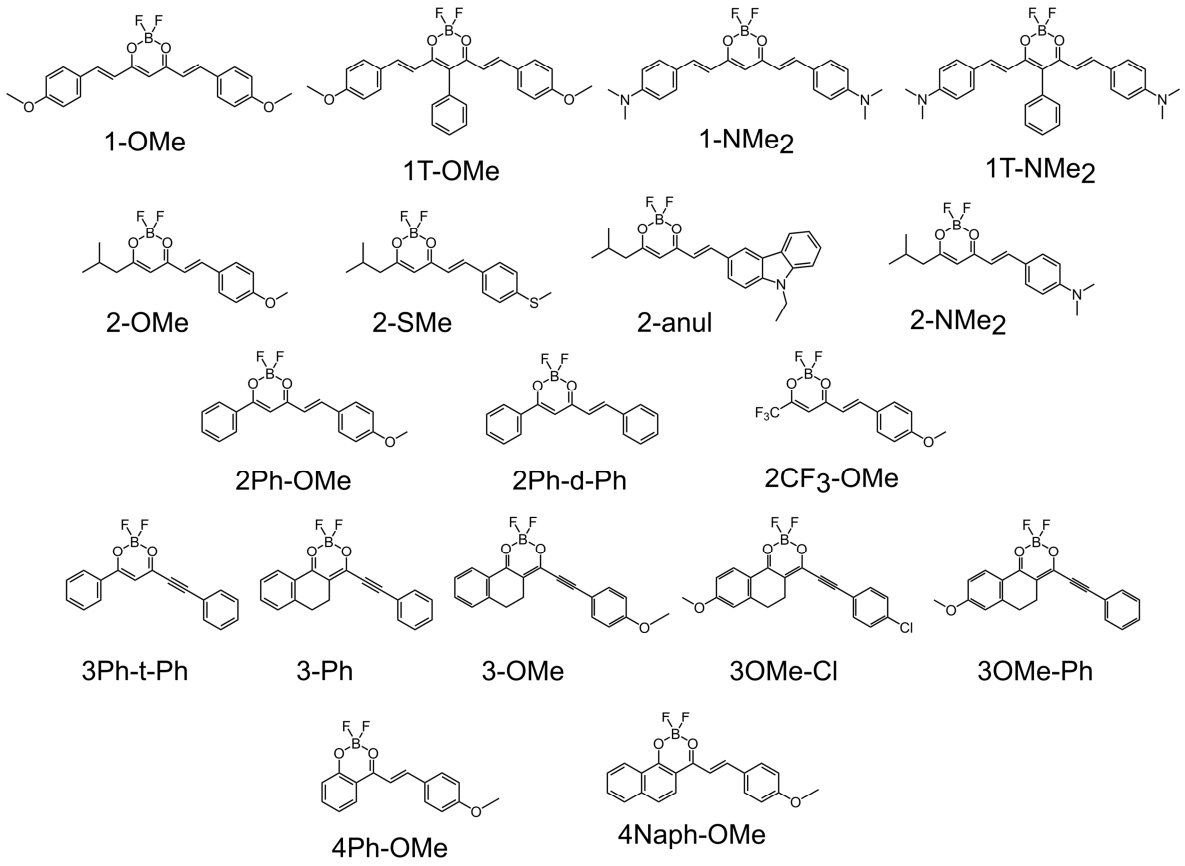

Scheme 2. Representation of the borondifluoride β-diketonate complexes studied in the present work.

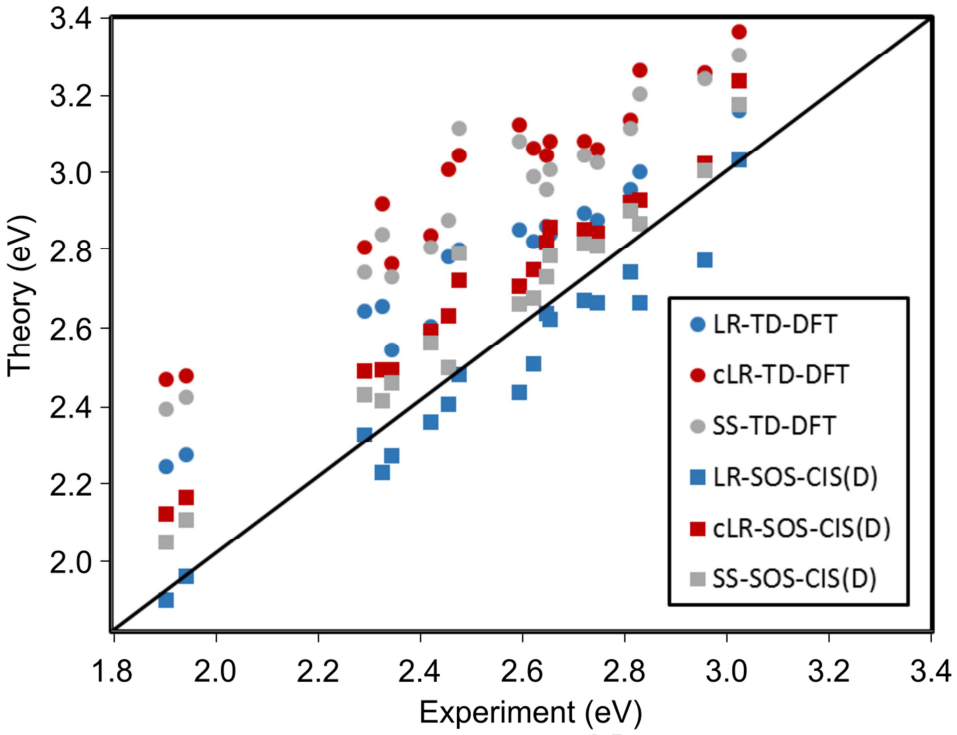

Figure 1. Comparison between theoretical (LR, cLR, SS, LR-SOS-CIS(D), cLR-SOS-CIS(D) and SS-SOS-CIS(D)) and experimental AFCP values (eV). The central line indicates a perfect theory-experiment match.

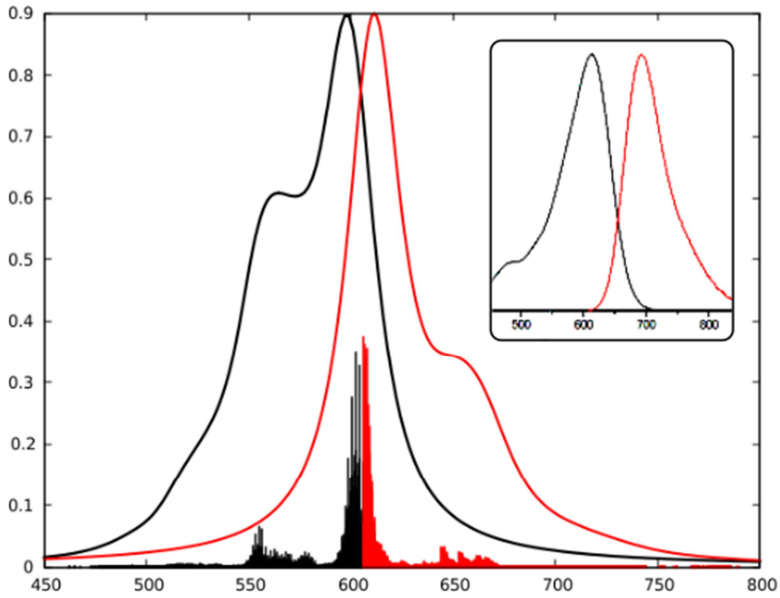

Figure 2. Comparison between the experimental (inset) and theoretical normalized absorption (black) and emission spectra (red) of **1T-NMe$_2$**, in solution. The experimental curve is adapted from Ref 40.

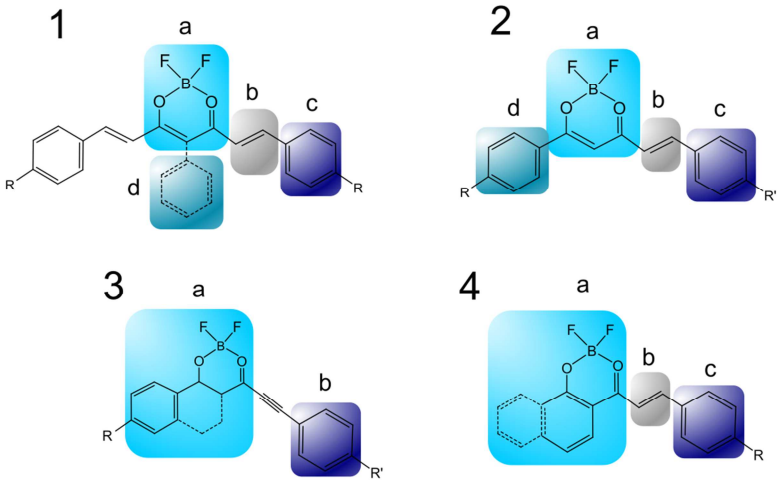

Figure 3. Structural planes for some selected chromophores representative of each family.

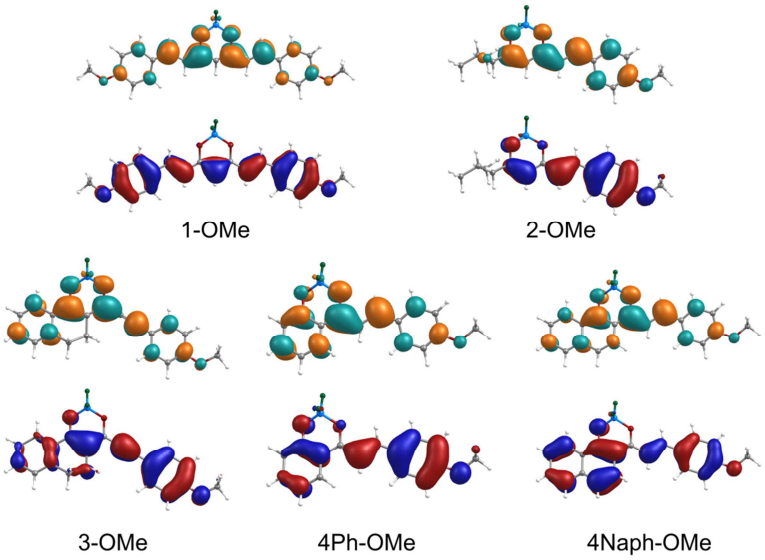

Figure 4. HOMO-LUMO plots for some selected chromophores. The HOMO is represented in red-blue, and the LUMO in turquoise-orange. A contour threshold of 0.03 a.u. has been considered.

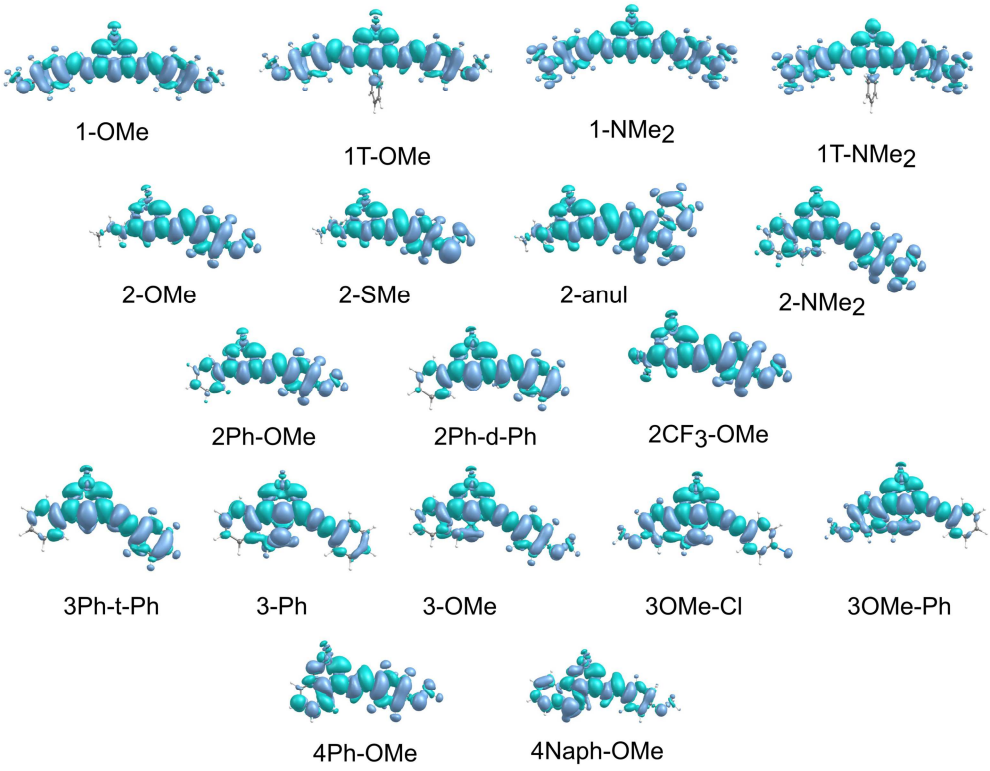

Figure 5. Electronic Density Difference plots for the studied systems. Turquoise and blue colors indicate charge accumulation and depletion, respectively. A contour threshold of 0.0004 a.u. has been considered.

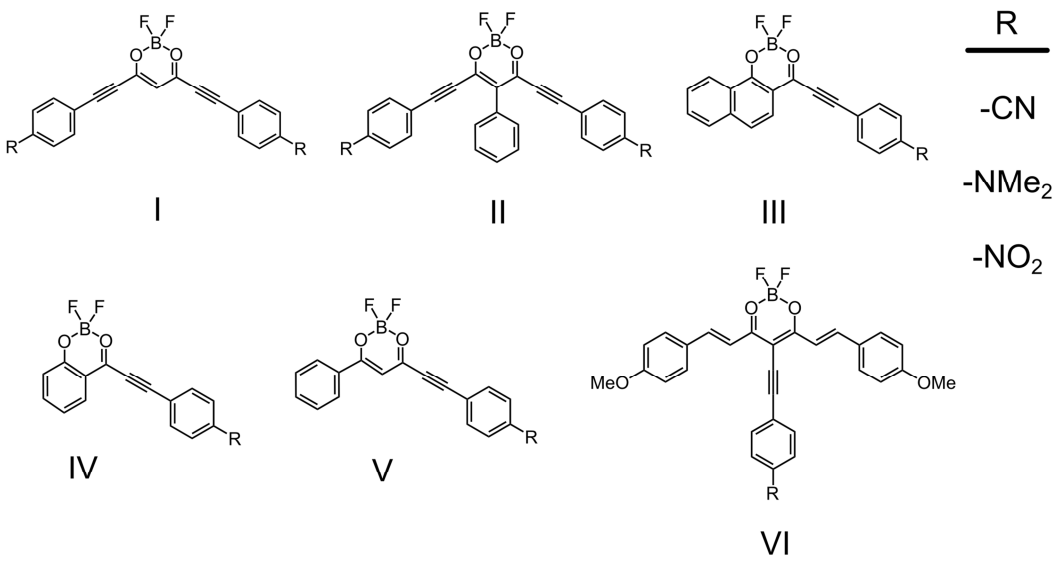

Scheme 3. Hypothetical borondifluoride *β*-diketonate complexes studied in the present work.

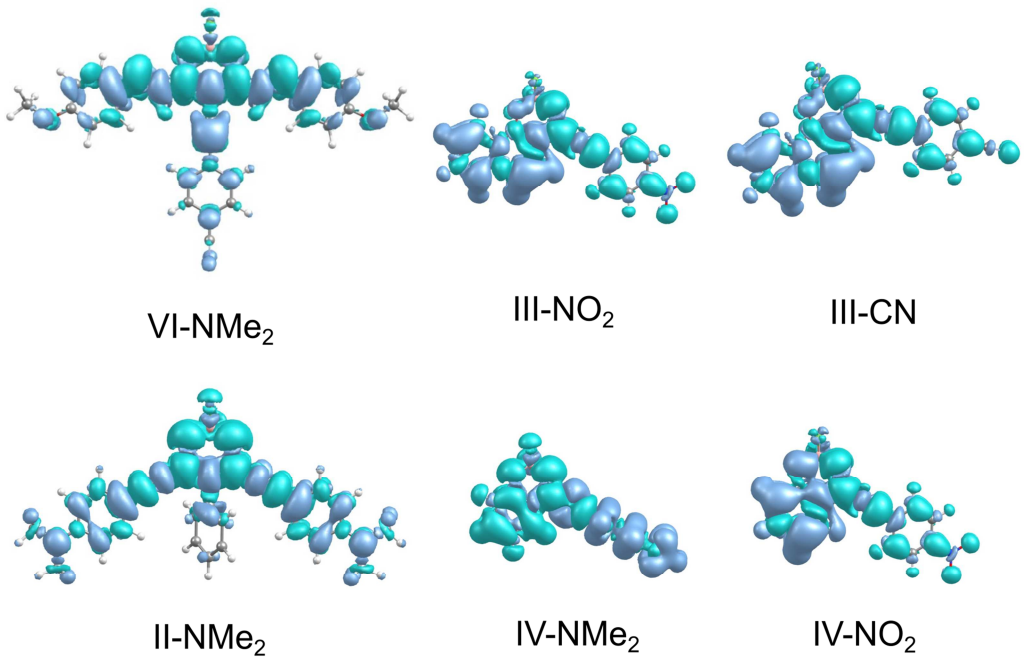

Figure 6. Electronic Density Difference plots for some of the hypothetical borondifluoride *β*-diketonate complexes. Turquoise and blue colors indicate charge accumulation and depletion, respectively. A contour threshold of 0.0004 a.u. has been considered.

BIBLIOGRAPHIC REFERENCES

[1] Kobayashi, H.; Ogawa, M.; Alford, R.; Choyke, P. L.; Urano, Y. New Strategies for Fluorescent Probe Design in Medical Diagnostic Imaging. *Chem. Rev.* **2010**, *12*, 2620-2640.

[2] Li, J.; Yim, D.; Jang, W.-D. ; Yoon, J. Recent Progress in the Design and Applications of Fluorescence Probes containing Crown Ethers. *Chem. Soc. Rev.* **2017**, *46*, 2437-2458.

[3] Tan, Y.; Liu, R.; Zhang, H.; Peltier, R.; Lam, Y.-W.; Zhu, Q.; Hu, Y.; Sun, H. Design and Synthesis of Near-Infrared Fluorescent Probes for Imaging of Biological Nitroxyl. *Sci. Rep.* **2015**, *5*, 16979.

[4] Garland, M.; Yim, J. J.; Bogyo, M. A Bright Future for Precision Medicine: Advances in Fluorescent Chemical Probe Design and their Clinical Application. *Cell Chem. Biol.* **2016**, *23*, 122-136.

[5] Yang, X.; Zhou, G.; Wong, W.-Y. Functionalization of Phosphorescent Emitters and their Host Materials by Main-group Elements for Phosphorescent Organic Light-emitting Materials. *Chem. Soc. Rev.* **2015**, *44*, 8484-8575.

[6] Fresta, E.; Costa, R. D. Beyond Traditional Light-emitting Electrochemical Cells – A Review of New Device Designs and Emitters. *J. Mater. Chem. C* **2017**, *5*, 5643-5675.

[7] Zhang, S.; Adhikari, R.; Fang, M.; Dorh, N.; Li, C.; Jaishi, M.; Zhang, J.; Tiwari, A.; Pati, R.; Luo, F.-T.; Liu, H. Near-Infrared Fluorescent Probes with Large Stokes Shifts for Sensing Zn(II) Ions in Living Cells. *ACS Sens.* **2016**, 1, 1408-1415.

[8]. Lou, Z.; Li, P.; Han, K. Redox-Responsive Fluorescent Probes with Different Design Strategies. *Acc. Chem. Res.* **2015**, *48*, 1358-1368.

[9] Murtagh, J.; Frimannsson, D. O.; O'Shea, D. F. Azide Conjugatable and pH Responsive Near-Infrared Fluorescent Imaging Probes. *Org. Lett.* **2009**, *11*, 5386-5389.

[10] D'Aléo, A.; Fages, F. Boron Complexes as Solid-State Fluorophores. *Display and Imaging* **2014**, *2*, 149-174.

[11] D'Aléo, A.; Felouat, A.; Fages, F. Boron Difluoride Complexes of 2'-Hydroxychalcones and Curcuminoids as Fluorescent Dyes for Photonic Applications. *Adv. Nat. Sci.: Nanosci. Nanotechnol.* **2015**, *6*, 015009.

[12] Bai, G.; Yu, C.; Cheng, C.; Hao, E.; Wei, Y.; Mu, X.; Jiao, L. Syntheses and Photophysical Properties of BF_2 Complexes of Curcumin Analogues. *Org. Biomol. Chem.* **2014**, *12*, 1618.

[13] Bañuelos, J. BODIPY Dye, the Most Versatile Fluorophore Ever? *Chem. Rec.* **2016**, *16*, 335-348.

[14] De Rosa, C. A.; Samonina-Kosicka, J.; Fan, Z.; Hendargo, H. C.; Weitzel, D. H.; Palmer, G. M.; Fraser, C. L. Oxygen Sensing Difluoroboron Dinaphthoyl methane Polylactide. *Macromolecules* **2015**, *48*, 2967-2977.

[15] Morris, W. A.; Liu, T.; Fraser, C. L. Mechanochromic Lumiscence of Halide-Substituted Difluoroboronβ-diketonate dyes. *J. Mater. Chem. C* **2015**, *3*, 352-363.

[16] Xu, S.; Evans, R. E.; Liu, T.; Zhang, G.; Demas, J. N.; Trindle, C. O.; Fraser, C. L. Aromatic Difluoroboronβ-Diketonate Complexes: Effects of π-Conjugation and Media on optical Properties. *Inorg. Chem.* **2013**, *52*, 3597-3610.

[17] Safonov, A. A.; Bagaturyants, A. A.; Sazhnikov, V. A. Fluorescence Spectra of (Dibenzoylmethanato)Boron Difluoride Exciplexes with Aromatic Hydrocarbons : A Theoretical Study. *J. Phys. Chem. A* **2015**, *119*, 8182-8187.

[18] D'Aleo, A.; Felouat, A.; Heresanu, V.; Ranguis, A.; Chaudanson, D.; Karapetyan, A.; Giorgi, M.; Fages, F. Two-photon Excited Fluorescence of BF_2 Complexes of Curcumin Analogues: Toward NIR-to-NIR Fluorescent Organic Nanoparticles. *J. Mater. Chem. C* **2014**, *2*, 5208-5215.

[19] Cogné-Laage, E.; Allemand, J.-F.; Ruel, O.; Baudin, J.-B.; Croquette, V.; Blanchard-Desce, M.; Jullien, L. Diaroyl(methanato)boron Difluoride Compounds as Medium-Sensitive Two-Photon Fluorescent Probes. *Chem. Eur. J.* **2004**, *10*, 1445-1455.

[20] Sun, L.; Zhang, F.; Wang, X.; Qiu, F.; Xue, M.; Tregnago, G.; Cacialli, F.; Osella, S.; Beljonne, D.; Feng, X. Geometric and Electronic Structures of Boron(III)-Cored Dyes Tailored by Incorporation of Heteroatoms into Ligands. *Chem. Asian J.* **2015**, *10*, 709-714.

[21] Kim, E.; Felouat, A.; Zaborova, E.; Ribierre, J.-C.; Wu, J. W.; Senatore, S.; Matthews, C.; Lenne, P.-F.; Baffert, C.; Karapetyan, A.; Giorgi, M.; Jacquemin, D.; Ponce-Vargas, M.; Le Guennic, B.; Fages, F.; D'Aléo, A. Borondifluoride Complexes of Hemicurcuminoids as Bio-Inspired Push-Pull Dyes for Bioimaging. *Org. Biomol. Chem.* **2016**, *14*, 1311-1324.

[22] Pantazis, P.; Supatto, W. Advances in Whole-EmbryoImaging: A Quantitative Transition is Underway. *Nature Rev. Mol. Cell Bio.* **2014**, *15*, 327-339.

[23] Reisfeld, R.; Shamrakov, D.; Jorgensen, C. Photostable Solar Concentrators based on Fluorescent Glass Films. *Sol. Energy Mat. Sol. Cells* **1994**, *33*, 417-427.

[24] Liu, W.; Zhou, B.; Niu, G.; Ge, J.; Wu, J.; Zhang, H.; Xu, H.; Wang, P. Deep-Red Emissive Crescent-Shaped Fluorescent Dyes: Substituent Effect on Live Cell Imaging. *ACS Appl. Mater. Interfaces* **2015**, *7*, 7421-7427.

[25] Wood, C. J.; Cheng, M.; Clark, C. A.; Horvath, R.; Clark, I. P.; Hamilton, M. L.; Towrie, M.; George, M. W.; Sun, L.; Yang, X.; Gibson, E. A. Red-Absorbing Cationic Acceptor Dyes for Photocathodes in Tandem Solar Cells. *J. Phys. Chem. C* **2014**, *118*, 16536-16546.

[26] Klymchenko, A. S.; Pivovarenko, V. G.; Ozturk, T.; Demchenko, A. P. Modulation of the solvent-dependent dual emission in 3-hydroxychromones by substituents. *New J. Chem.* **2003**, *27*, 1336-1343.

[27] Benniston, A. C.; Winstanley, T. P. L.; Lemmetyinen, H.; Tkachenko, N. V.; Harrington, R. W.; Wills, C. Large Stokes Shift Fluorescent Dyes Based on a Highly Substituted Terephthalic Acid Core. *Org. Lett.* **2012**, *14*, 1374-1377.

[28] Chen, Y.; Zhao, J.; Guo, H.; Xie, L. Geometry Relaxation-Induced Large Stokes Shift in Red-Emitting Borondipyrromethenes (BODIPY) and Applications in Fluorescent Thiol Probes. *J. Org. Chem.* **2012**, *77*, 2192-2206.

[29] Leen, V.; Miscoria, D.; Yin, S.; Filarowski, A.; Ngongo, J. M.; Van der Auweraer, M.; Boens, N.; Dehaen, W. 1,7-Disubstituted Boron Dipyrromethene (BODIPY) Dyes: Synthesis and Spectroscopic Properties. *J. Org. Chem.* **2011**, *76*, 8168-8176.

[30] Le Guennic, B.; Jacquemin, D. Taking Up the Cyanine Challenge with Quantum Tools. *Acc. Chem. Res.* **2015**, *48*, 530-537.

[31] Head-Gordon, M.; Rico, R. J.; Oumi, M.; Lee, T. J. A Doubles Correction to Electronic Excited States from Configuration Interaction in the Space of Single Substitutions. *Chem. Phys. Lett.* **1994**, *219*, 21-29.

[32] Rhee, Y. M.; Head-Gordon, M. Scaled Second-order Perturbation Corrections to Configuration Interaction Singles: Efficient and Reliable Excitation Energy Methods. *J. Phys. Chem. A* **2007**, *111*, 5314-5326.

[33] Dreuw, A.; Wormit, M. The Algebraic Diagrammatic Construction Scheme for the Polarization Propagator for the Calculation of Excited States. WIREs Comput. *Mol. Sci.* **2015**, *5*, 82-95.

[34] Christiansen, O.; Koch, H.; Jørgensen, P. The Second-Order Approximate Coupled Cluster Singles and Doubles Model CC2. *Chem. Phys. Lett.* **1995**, *243*, 409-418.

[35] Ishikawa, N.; Head-Gordon, M. Analytical Gradient of the CIS(D) Perturbative Correction to Single-Excitation Configuration Interaction Excited States. *Int. J. Quantum. Chem.* **1995**, *56*, 421-427.

[36] Chibani, S.; Laurent, A.; Le Guennic, B.; Jacquemin, D. Improving the Accuracy of Excited-State Simulations of BODIPY and Aza-BODIPY Dyes with a Joint SOS-CIS(D) and TD-DFT Approach. *J. Chem. Theory Comput.* **2014**, *10*, 4574-4582.

[37] Charaf-Eddin, A.; Le Guennic, B.; Jacquemin, D. Excited-states of BODIPY-cyanines: ultimate TD-DFT challenges? *RSC Adv.* **2014**, *4*, 49449-49456.

[38] Chibani, S.; Laurent, A. D.; Le Guennic, B.; Jacquemin, D. Excited States of Ladder-Type π-Conjugated Dyes with a Joint SOS-CIS(D) and PCM-TD-DFT Approach. *J. Phys. Chem. A* **2015**, *119*, 5417, 5425.

[39] Ponce-Vargas, M.; Azarias, C.; Jacquemin, D.; Le Guennic, B. Combined TD-DFT-SOS-CIS(D) Study of BOPHY Derivatives with Potential Application in Biosensing. *J. Phys. Chem. B* **2017**, *121*,10850-10858.

[40] Canard, G.; Ponce-Vargas, M.; Jacquemin, D.; Le Guennic, D.; Felouat, A.; Rivoal, M.; Zaborova, E.; D'Aléo, A.; Fages, F. Influence of the Electron Donor Groups on the Optical and Electrochemical Properties of Borondifluoride Complexes of Curcuminoid Derivatives: A Joint Theoretical and Experimental Study. *RSC Adv.* **2017**, *7*, 10132-10142. The experimental spectrum of Figure 4 has been published by The Royal Society of Chemistry (RSC).

[41] Štefane, B.; Požgan, F.; Kim, E.; Choi, E.; Ribierre, J.-C.; Wu, J. W.; Ponce-Vargas, M.; Le Guennic, B.; Jacquemin, D.; Canard, G.; Zaborova, E.; Fages, F.; D'Aléo, A. Ethylene-Analogues of Hemicurcuminoids: Synthesis and Ground and Excited Properties of their Boron Difluoride Complexes. *Dyes Pigm.* **2017**, *141*, 38-47.

[42] Kamada, K.; Namikawa, T.; Senatore, S.; Matthews, C.; Lenne, P.-F.; Maury, O.; Andraud, C.; Ponce-Vargas, M.; Le Guennic, B.; Jacquemin, D.; Agbo, P.; An, D. D.; Gauny, S. S.; Liu, X.; Abergel, R. J.; Fages, F.; D'Aléo, A. Boron Difluoride Curcuminoid

Fluorophores with Enhanced Two-Photon Excited Fluorescence Emission and Versatile Living-Cell Imaging Properties. *Chem. Eur. J.* **2016**, *22*, 5219-5232.

[43] D'Aléo, A.; Gachet, D.; Heresanu, V.; Giorgi, M.; Fages, F. Efficient NIR-Light Emission from Solid-State Complexes of BoronDifluoride with 2'-Hydroxychalcone Derivatives. *Chem. Eur. J.* **2012**, *18*, 12764-12772.

[44] Chambon, S.; D'Aléo, A.; Baffert, C.; Wantz, G.; Fages, F. Solution-Processed Bulk Heterojunction Solar Cells based on BF_2-Hydroxychalcone Complexes. *Chem. Commun.* **2013**, *49*, 3555-3557.

[45] Reyes, H.; García, M. C.; Flores, B. M.; López-Rebolledo, H.; Santillán, R.; Farfán, N. Synthesis, NMR and X-Ray Diffraction Analysis of Boron Complexes Derived from Hydroxychalcones. *J. Mex. Chem. Soc* .**2006**, *50*, 106-113.

[46] Gaussian 09. Revision D. 01. Frisch, M. J. et al. Gaussian Inc., Wallingford CT, **2009**.

[47] Zhao, Y.; Truhlar, D. G. The M062 Suite of Density Functionals for Main Group Thermochemistry, Thermochemical Kinetics, Non-covalent Interactions, Excited States, and Transition Elements: Two New Functionals and Systematic Testing of Four M062-Class Functionals and 12 Other Functionals. *Theor. Chem. Acc.* **2008**, *120*, 215-241.

[48] Tomasi, J.; Mennucci, B.; Cammi, R. Quantum Mechanical Continuum Solvation Models. *Chem. Rev.* **2005**, *105*, 2999-3093.

[49] Mennucci, B.; Tomasi, J.; Cammi, R.; Cheeseman, J. R.; Frisch, M. J.; Devlin, F. J.; Gabriel, S.; Stephens, P. J. Polarizable Continuum Model (PCM) Calculations of Solvent Effects on Optical Rotations of Chiral Molecules. *J. Phys. Chem. A* **2002**, *106*, 6102-6113.

[50] Curutchet, C.; Muñoz-Losa A.; Monti, S.; Kongsted, J.; Scholes, G. D.; Mennucci, B. Electronic Energy Transfer in Condensed Phase Studied by a Polarizable QM/MM Model. *J. Chem. Theory Comput.* **2009**, *5*, 1838-1848.

[51] Cammi, R.; Mennucci, B. Linear Response Theory for the Polarizable Continuum Model. *J. Chem. Phys.* **1999**, *110*, 9877-9886.

[52] Cossi, M.; Barone, V. Time-Dependent Density Functional Theory for Molecules in Liquid Solutions. *J. Chem. Phys.* **2001**, *115*, 4708-4717.

[53] Improta, R.; Scalmani, G.; Frisch, M. J.; Barone, V. Toward Effective and Reliable Fluorescence Energies in Solution by a New State Specific Polarizable Continuum Model Time Dependent Density Functional Theory Approach. *J. Chem. Phys.* **2007**, *127*, 074504.

[54] Caricato, M.; Mennucci, B.; Tomasi, J.; Ingrosso, F.; Cammi, R.; Corni, S.; Scalmani, G. Formation and Relaxation of Excited States in Solution: A New Time Dependent Polarizable Continuum Model based on Time Dependent Density Functional Theory. *J. Chem. Phys.* **2006**, *124*, 124520.

[55] Shao, Y. Gan, Z.; Epifanovsky, E.; et al. Advances in Molecular Quantum Chemistry contained in the Q-Chem 4 Program Package. *Mol. Phys.* **2015**, *113*, 184-215.

[56] Santoro, F.; Improta, R.; Lami, A.; Bloino, J.; Barone, V. Effective method to compute Franck-Condon integrals for optical spectra of large molecules in solution. *J. Chem. Phys.* **2007**, *126*, 084509.

[57] Santoro, F.; Lami, A.; Improta, R.; Barone, V. Effective method to compute vibrationally resolved spectra of large molecules at finite temperature in the gas phase and in solution. *J. Chem. Phys.* **2007**, *126*, 184102.

[58] Santoro, F.; Lami, A.; Improta, R.; Bloino, J.; Barone, V. Effective method for the computation of optical spectra of large molecules at finite temperature including the Duschinsky and Herzberg-Teller effect: The Q_x band of porphyrin as a case study. *J. Chem. Phys.* **2008**, *128*, 224311.

[59] Santoro, F. "FCclasses, a fortran 77 code": http://village.ipcf.cnr.it..

[60] Andrienko, G. http://www.chemcraftprog.com.

[61] Le Bahers, T.; Adamo, C.; Ciofini, I. A qualitative Index of Spatial Extent in Charge-transfer Excitations. *J. Chem. Theory Comput.* **2011**, *7*, 2498-2506.

[62] Jacquemin, D.; Le Bahers, T.; Adamo, C.; Ciofini, I. What is the "best" atomic charge model to describe through-space charge-transfer excitations? *Phys. Chem. Chem. Phys.* **2012**, *14*, 5383-5388.

[63] Bureš, F.; Čermáková, H; Kulhánek, J.; Ludwig, M.; Kuznik, W.; Kityk, I. V.; Mikysek, T.; Růžička, A. Structure-Property Relationships and Nonlinear Optical Effects in Donor-Substituted Dicyanopyrazine-Derived Push-Pull Chromophores with Enlarged and Varied π-Linkers. *Eur. J. Org. Chem.* **2012**, 529-538.

GRAPHICAL TABLE OF CONTENTS (TOC)